

# Supporting Information

Takamatsu et al. 10.1073/pnas.1712263115

## SI Experimental Procedures

**Cells and Viruses.** Huh-7 (human hepatoma), HEK293 (human embryonic kidney), VeroE6 (African green monkey kidney) cells were maintained in DMEM (Life Technologies) supplemented with 10% (vol/vol) FBS (PAN Biotech), 5 mM L-glutamine (Q; Life Technologies), 50 U/mL penicillin, and 50  $\mu$ g/mL streptomycin (PS; Life Technologies) and grown at 37 °C with 5% CO<sub>2</sub>. During live-cell imaging, cells were cultivated in Leibovitz's medium (Life Technologies) with PS/Q, nonessential amino acid solution, and 20% (vol/vol) FBS. The recombinant virus used in this study was based on EBOV Zaire (strain Mayinga; GenBank accession no. AF272001). Cloning and rescue of full-length EBOV was performed as described previously (1, 2). All work with infectious viruses was performed in the BSL-4 facility at the Philipps-University Marburg.

**Molecular Cloning and Plasmids.** All plasmids coding for wild-type EBOV proteins (pCAGGS-NP, pCAGGS-VP35, pCAGGS-VP40, pCAGGS-GP, pCAGGS-VP30, pCAGGS-VP24, pCAGGS-L), as well as T7-driven minigenome encoding a *Renilla* luciferase reporter, and pCAGGS-T7 polymerase have been used as described previously (3, 4). Generation procedure of the plasmid pCAGGS-VP30-GFP coding for the VP30-GFP fusion protein: The GFP ORF was cloned in frame to the 3' end of the VP30 gene as previously described (5–8). Construction of the pCAGGS-VP24-TagRFP, pCAGGS-VP35-GFP, pCAGGS-VP40-TagRFP, pCAGGS-NP-TagRFP was achieved by using ligation-PCR technique enabled to include GS Linker with Phusion High-Fidelity DNA Polymerase (New England Biolabs). Resulting constructs were subcloned into pCAGGS (9, 10) using XmaI and NotI (VP24-TagRFP, VP40-TagRFP, NP-TagRFP), or XmaI and NheI (VP35-GFP). All constructs were verified by DNA sequencing. Primers sequences are available in Table S1.

**Minigenome and trVLP Reporter Assay.** Minigenome assay was performed as described previously (11). Briefly, the plasmids for minigenome assay (125 ng of pCAGGS-NP, 125 ng of pCAGGS-VP35, 100 ng of pCAGGS-VP30, 1,000 ng of pCAGGS-L, 250 ng of a EBOV-specific minigenome encoding the *Renilla* luciferase reporter gene, and 250 ng of the pCAGGS-T7 polymerase) with or without pCAGGS-VP24/pCAGGS-VP40 were transfected in HEK293 cells. Reporter activity was measured at 48 h posttransfection. The DNA amount of 100 ng was used for pCAGGS-VP30 and pCAGGS-VP24 transfection, instead of 75 ng for pCAGGS-VP30 and 60 ng for pCAGGS-VP24 reported previously (11). For analysis of transcription/replication activity, the EBOV trVLP assay was performed as described previously (4, 12), with small modifications. Briefly, HEK293 cells were transfected with plasmids encoding all EBOV structural proteins (125 ng of pCAGGS-NP, 125 ng of pCAGGS-VP35, 250 ng of pCAGGS-VP40, 250 ng of pCAGGS-GP, 100 ng of pCAGGS-VP30, 100 ng of pCAGGS-VP24, 1,000 ng of pCAGGS-L), 250 ng of a EBOV-specific minigenome, and 250 ng of pCAGGS-T7 polymerase. Culture supernatants were collected at 72 h posttransfection, and trVLPs were purified via ultracentrifugation through a 20% sucrose cushion.

**Antibodies.** The following primary antibodies were used for immunofluorescent analysis: a chicken anti-NP polyclonal antibody (13), a rabbit anti-HA antibody (Rockland), and a rabbit anti-VP30 antibody (3). Corresponding secondary antibodies, donkey anti-chicken-IRDye680RD (Li-COR), goat anti-chicken IgY DyLight 488 (Abcam), and goat anti-rabbit-IRDye680RD (Li-COR) were

used. The following primary antibodies were used for Western blot analysis: a chicken anti-NP polyclonal antibody (13), a mouse monoclonal VP35 [6C5] antibody (Kerafast), a mouse monoclonal anti-VP40 (14), a guinea pig anti-VP30 antibody (3), a rabbit anti-VP24 antibody [a kind gift from Viktor Volchkov, University Claude Bernard, INSERM U412, Lyon, France (15)], a goat anti-GFP antibody (Rockland), a rabbit anti-trRFP (TagRFP) antibody (Evrogen), a mouse anti-Flag M2 monoclonal antibody (Sigma-Aldrich), a mouse anti- $\alpha$ -tubulin antibody (Abcam), and a mouse anti- $\beta$ -actin antibody (Abcam). Corresponding secondary antibodies were: donkey anti-chicken IRDye 680RD (Li-COR), donkey anti-chicken-IRDye 800CW (Li-COR), donkey anti-guinea pig IRDye 800CW (Li-COR), donkey anti-goat Alexa Fluor 680 (Invitrogen), donkey anti-goat IRDye800 (Rockland), goat anti-rabbit IRDye 680RD (Li-COR), donkey anti-rabbit IRDye 680RD (Li-COR), swine polyclonal anti-rabbit immunoglobulins/HRP (Dako), donkey anti-rabbit IRDye 800CW (Li-COR), donkey anti-mouse 680RD (Li-COR), goat anti-mouse IRDye 800CW (Li-COR), and donkey anti-mouse IRDye 800CW (Li-COR).

**Immunofluorescence Analysis and Confocal Laser Scanning Microscopy.** Immunofluorescence analysis was performed as described previously (16, 17). The microscopic images were acquired by Leica SP5 confocal laser scanning microscope using a 63 $\times$  oil objective (Leica Microsystems). Cells were grown on glass coverslips and fixed with 4% paraformaldehyde at 20 h posttransfection. Optionally, a nucleus staining was achieved by using DAPI.

**Immunoprecipitation Analysis.** Immunoprecipitation analysis was performed as described previously (3). The eluted samples were subjected to SDS-PAGE and Western blot analysis.

**SDS-PAGE and Western Blot Analysis.** SDS-PAGE and Western Blot analysis were performed as described previously (3, 18). The protein detection was performed with Image Lab software for HRP-conjugated secondary antibodies or Li-Cor Odyssey imaging system for fluorescent conjugated secondary antibodies as indicated in the antibodies section.

**Infection and Transfection of Cells in BSL-4.** Huh-7 cells grown on  $\mu$ -Slide 8-well (Ibidi) were infected at a multiplicity of infection of 1 in a volume of 250  $\mu$ L DMEM/PS/Q without FBS. The inoculum was removed 1 h after infection, and 250  $\mu$ L of fresh DMEM/PS/Q without FBS were added to the cells. Subsequently, 500 ng of DNA encoding fluorescent fusion protein was transfected. One hour after transfection, the medium was removed and appropriate cell-culture medium was added.

**Live-Cell Microscopy.** For live-cell imaging,  $1 \times 10^4$  of Huh-7 cells were seeded onto  $\mu$ -Slide 8-well (Ibidi) and cultivated in DMEM/PS/Q with 10% FBS. The transfection was performed in 50  $\mu$ L Opti-MEM without phenol red (Life Technologies). The inoculum was removed at 1 h posttransfection, and added a volume of 250  $\mu$ L CO<sub>2</sub>-independent Leibovitz's medium (Life Technologies). Live-cell time-lapse experiments were recorded with Nikon ECLIPSE TE2000-E using a 63 $\times$  oil objective in the BSL-2, and with Leica DMI6000B in the BSL-4 using a 63 $\times$  oil objective equipped with a remote-control device to operate the microscope from outside the BSL-4 facility (9). Pictures and movie sequences were processed with the Nikon NIS Elements 4.1 software, or Leica Application Suite X software, respectively (9, 10).

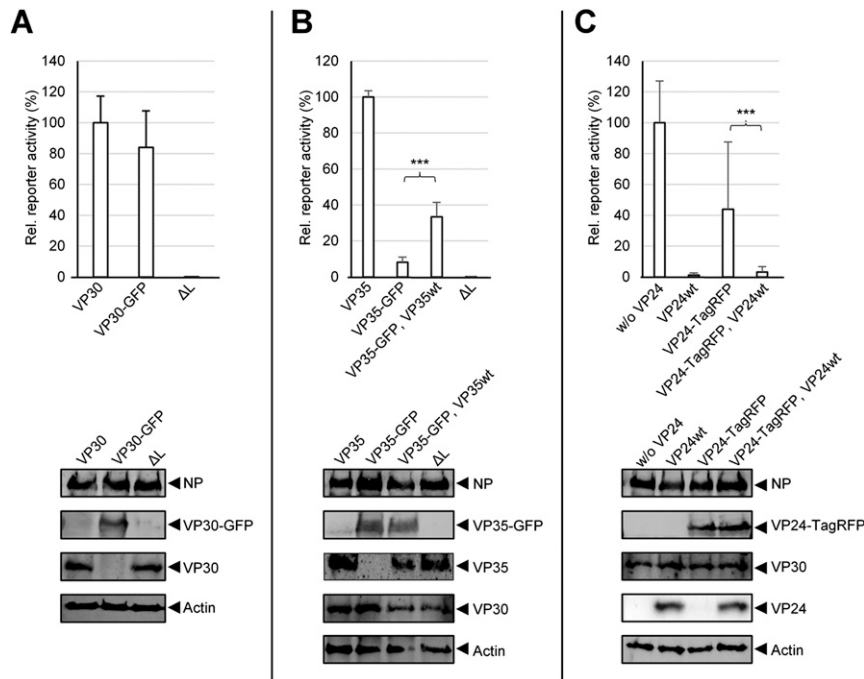
**Correlative Confocal and Electron Microscopy of trVLPs.** We performed correlative confocal and electron microscopy analyses of incorporation of the fluorescent fusion proteins into NCLSs. The trVLPs purified from the supernatant of HEK293 cells transfected with plasmids encoding VP30-GFP, VP24-TagRFP, and NP, L, VP35, VP24, VP40, GP, minigenome, T7 polymerase (Fig. 1F) were adsorbed on Finder grids. The position of VP30-GFP<sup>+</sup> and VP24-TagRFP<sup>+</sup> particles was first recorded by confocal microscopy, then the negatively stained with 2% phosphotungstic acid samples were analyzed by using JEM1400 transmission electron microscope.

**Treatment of Cells with Cytoskeleton-Modulating Drugs.** Cells were treated with 15  $\mu$ M nocodazole (Sigma), 0.3  $\mu$ M cytochalasin D

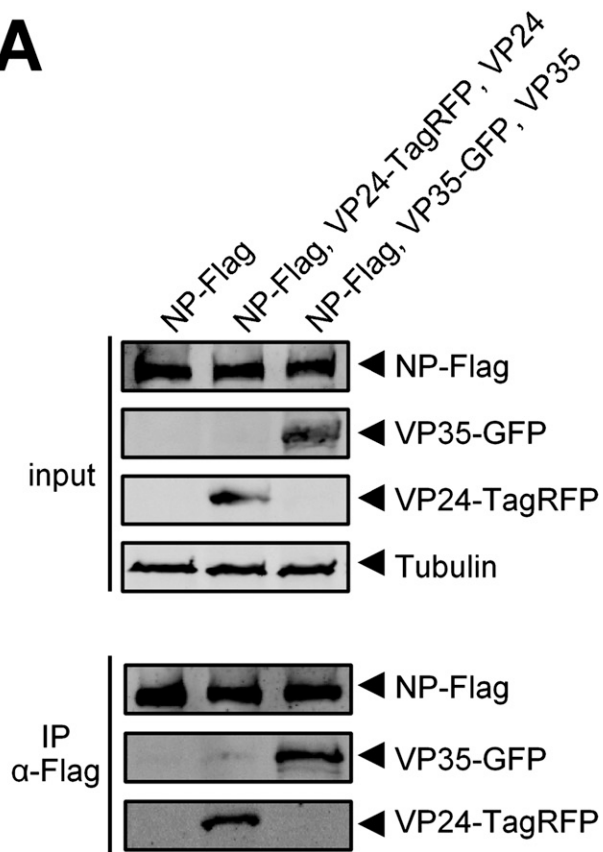
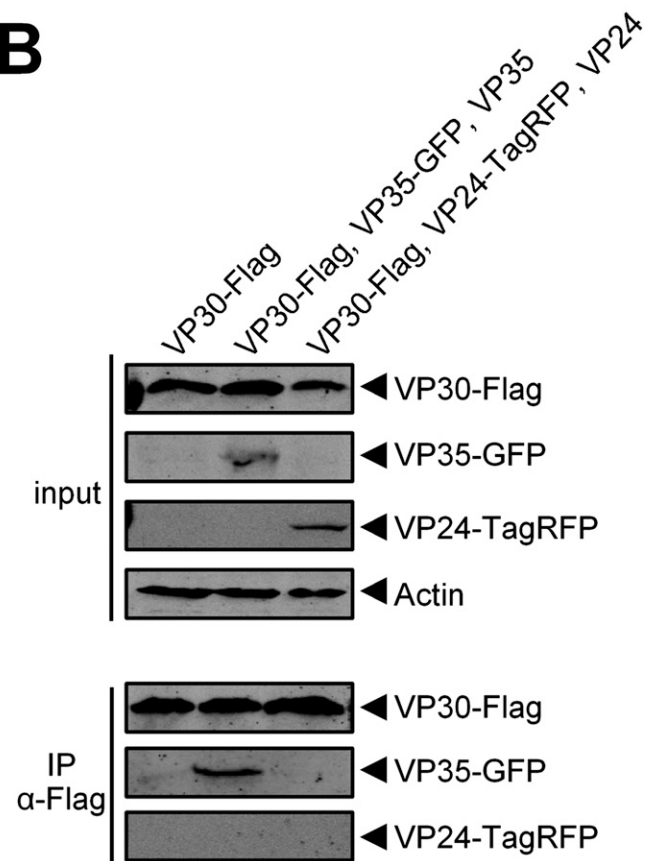
(Sigma), or 0.15% dimethyl sulfoxide (DMSO; Sigma) (5, 9). Chemicals were added to the cell culture medium 3 h before fluorescence microscopy was performed. For each tested inhibitor, more than 30 different cells with more than 20 NCLSs inside were analyzed.

**Statistical Analysis.** The presented data represent the median values and SDs from at least three independent experiments. Statistical analysis was performed by using SPSS16.0. Normally distributed samples were analyzed by *t* test, and the other samples were analyzed by nonparametric test. Statistically significant differences are indicated with asterisks (\* $P < 0.05$ ; \*\* $P < 0.01$ ; \*\*\* $P < 0.001$ ).

1. Groseth A, et al. (2012) The Ebola virus glycoprotein contributes to but is not sufficient for virulence in vivo. *PLoS Pathog* 8:e1002847.
2. Hoenen T, et al. (2012) Inclusion bodies are a site of ebolavirus replication. *J Virol* 86:11779–11788.
3. Biedenkopf N, Hartlieb B, Hoenen T, Becker S (2013) Phosphorylation of Ebola virus VP30 influences the composition of the viral nucleocapsid complex: Impact on viral transcription and replication. *J Biol Chem* 288:11165–11174.
4. Hoenen T, et al. (2006) Infection of naive target cells with virus-like particles: Implications for the function of Ebola virus VP24. *J Virol* 80:7260–7264.
5. Schudt G, et al. (2015) Transport of Ebolavirus nucleocapsids is dependent on actin polymerization: Live-cell imaging analysis of Ebolavirus-infected cells. *J Infect Dis* 212(Suppl 2):S160–S166.
6. Bamberg S, Kolesnikova L, Möller P, Klenk HD, Becker S (2005) VP24 of Marburg virus influences formation of infectious particles. *J Virol* 79:13421–13433.
7. Mittler E, Kolesnikova L, Herwig A, Dolnik O, Becker S (2013) Assembly of the Marburg virus envelope. *Cell Microbiol* 15:270–284.
8. Krähling V, et al. (2010) Establishment of fruit bat cells (*Rousettus aegyptiacus*) as a model system for the investigation of filoviral infection. *PLoS Negl Trop Dis* 4:e802.
9. Schudt G, Kolesnikova L, Dolnik O, Sodeik B, Becker S (2013) Live-cell imaging of Marburg virus-infected cells uncovers actin-dependent transport of nucleocapsids over long distances. *Proc Natl Acad Sci USA* 110:14402–14407.
10. Dolnik O, et al. (2014) Interaction with Tsg101 is necessary for the efficient transport and release of nucleocapsids in marburg virus-infected cells. *PLoS Pathog* 10:e1004463.
11. Hoenen T, Jung S, Herwig A, Groseth A, Becker S (2010) Both matrix proteins of Ebola virus contribute to the regulation of viral genome replication and transcription. *Virology* 403:56–66.
12. Biedenkopf N, Hoenen T (2017) Modeling the Ebolavirus life cycle with transcription and replication-competent viruslike particle assays. *Methods Mol Biol* 1628:119–131.
13. Biedenkopf N, Lier C, Becker S (2016) Dynamic phosphorylation of VP30 is essential for Ebola virus life cycle. *J Virol* 90:4914–4925.
14. Hoenen T, et al. (2005) VP40 octamers are essential for Ebola virus replication. *J Virol* 79:1898–1905.
15. Mateo M, et al. (2011) VP24 is a molecular determinant of Ebola virus virulence in Guinea pigs. *J Infect Dis* 204(Suppl 3):S1011–S1020.
16. Dolnik O, Kolesnikova L, Stevermann L, Becker S (2010) Tsg101 is recruited by a late domain of the nucleocapsid protein to support budding of Marburg virus-like particles. *J Virol* 84:7847–7856.
17. Kolesnikova L, Mittler E, Schudt G, Shams-Eldin H, Becker S (2012) Phosphorylation of Marburg virus matrix protein VP40 triggers assembly of nucleocapsids with the viral envelope at the plasma membrane. *Cell Microbiol* 14:182–197.
18. Kolesnikova L, Berghöfer B, Bamberg S, Becker S (2004) Multivesicular bodies as a platform for formation of the Marburg virus envelope. *J Virol* 78:12277–12287.



**Fig. S1.** Functional analysis of VP30-GFP, VP35-GFP, and VP24-TagRFP by using minigenome assay. (A and B) HEK293 cells were transfected with plasmids encoding the EBOV minigenome assay components (NP, VP35, VP30, L, the EBOV-specific minigenome, and T7 polymerase), a plasmid encoding one of the fluorescent fusion proteins was used either instead or in combination with plasmid encoding the corresponding wild-type nucleocapsid protein, as indicated. At 48 h posttransfection, the cells were lysed and the reporter gene activity was measured. The reporter gene activity was set to 100% when wild-type VP30 or VP35 was expressed (positive control). The negative control was without expression of L (ΔL) and displayed the background of the assay. (C) HEK293 cells were transfected with plasmids encoding NP, VP35, VP30, L, the EBOV-specific minigenome and T7 polymerase, and plasmids encoding either wild-type VP24 or VP24-TagRFP, or their mixture. At 48 h posttransfection, the cells were lysed and the reporter gene activity was measured. The reporter gene activity was set to 100% when wild-type VP24 was not expressed (positive control). Shown (Upper) are the medians and the SDs of the results of three independent experiments.  $***P < 0.001$ . Shown (Lower) is control for protein expression. Western blot analysis was performed using NP-, GFP-, VP30-, and β-actin-specific antibodies (A); NP-, GFP-, VP35-, VP30-, and β-actin-specific antibodies (B); and NP-, TagRFP-, VP30-, VP24-, and β-actin-specific antibodies (C).

**A****B**

**Fig. S2.** Interaction analysis of fluorescently labeled nucleocapsid proteins. (A) HEK293 cells were transfected with plasmids encoding Flag-tagged NP and empty vector, or VP24-TagRFP and VP24, or VP35-GFP and VP35. At 48 h posttransfection, the cells were lysed and protein complexes were precipitated using mouse anti-Flag M2 agarose. An aliquot of cell lysate (input) was collected before precipitation. Western blot analysis was performed using Flag-, GFP-, TagRFP-, and  $\alpha$ -tubulin-specific antibodies. (B) HEK293 cells were transfected with plasmids encoding Flag-tagged VP30 and empty vector, or VP35-GFP and VP35, or VP24-TagRFP and VP24. At 48 h posttransfection, the cells were lysed and protein complexes were precipitated using mouse anti-Flag M2 agarose. Western blot analysis was performed using Flag-, GFP-, TagRFP-, and  $\beta$ -actin-specific antibodies.

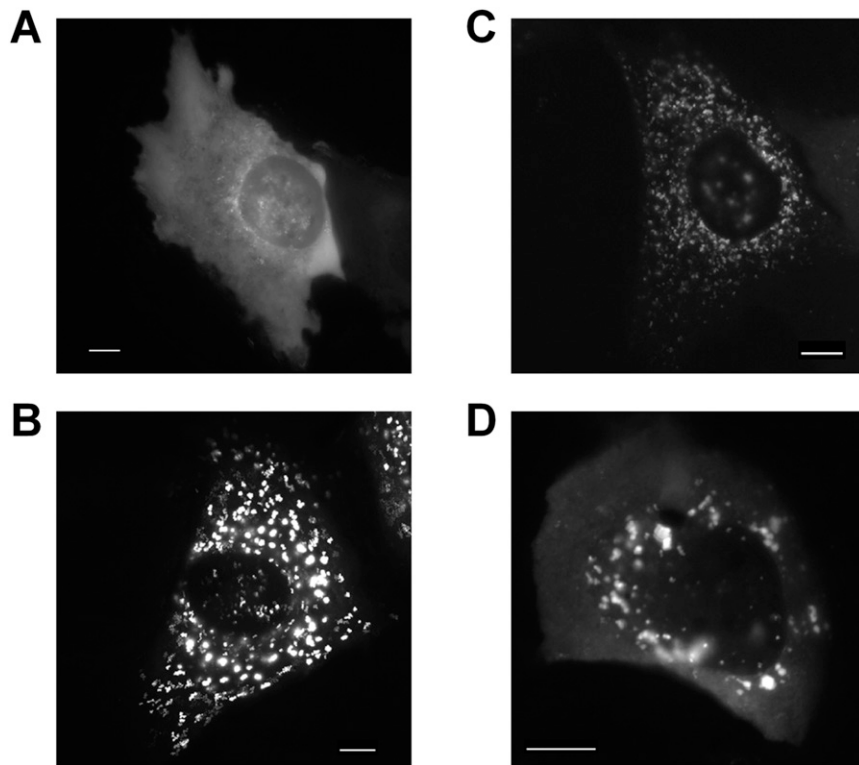


**Fig. 53.** Live-cell imaging analysis of singly expressed fluorescent nucleocapsid proteins. Huh-7 cells were transfected with plasmids encoding either VP30-GFP (A), or VP35-GFP and VP35 (B), or VP24-TagRFP and VP24 (C), or NP-TagRFP and NP (D). Live-cell imaging analysis was performed at 20 h posttransfection. Pictures show the maximum-intensity projection of time-lapse images of cells recorded for 2 min; one frame was taken every 2 s. (Scale bars, 10  $\mu$ m.)





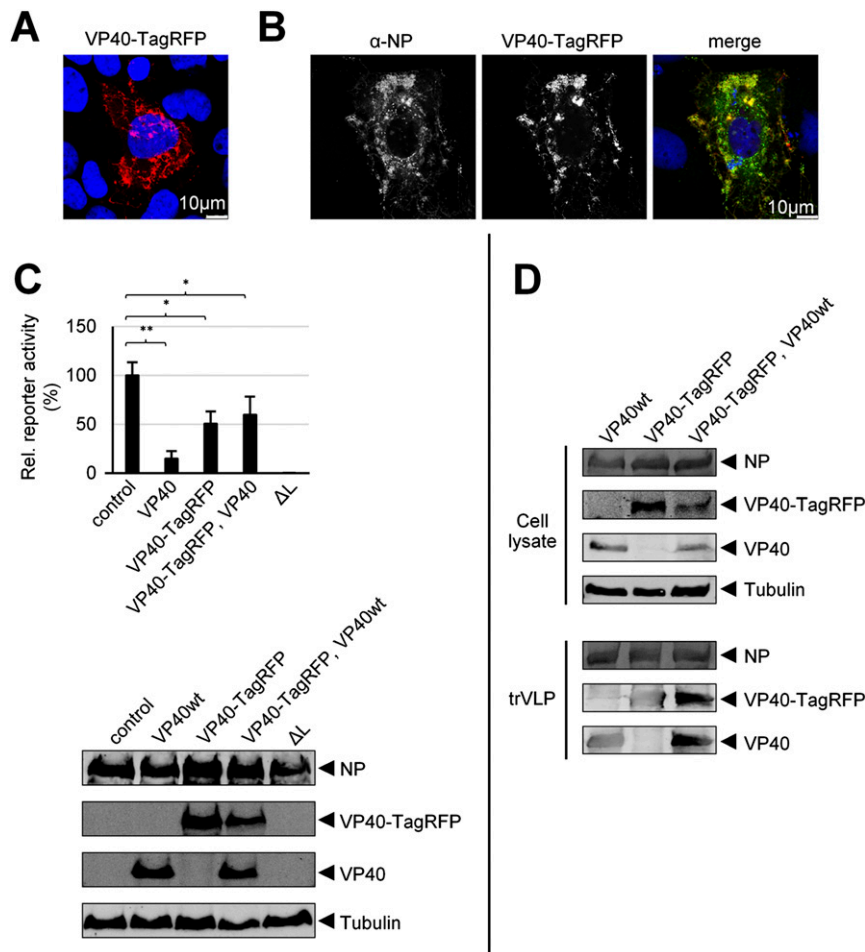
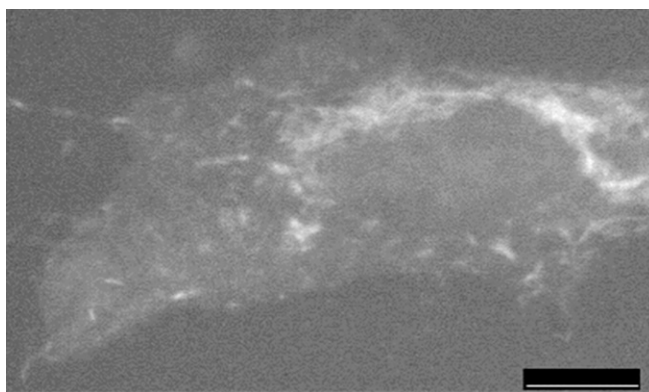


**Fig. S5.** Functional analysis of VP40-TagRFP by using confocal microscopy, minigenome, and trVLP assays. (*A* and *B*) Huh-7 cells were transfected with plasmids encoding VP40-TagRFP and VP40 (*A*), or with plasmids encoding VP40-TagRFP and components of trVLP assay. (*B*) Cells were fixed at 24 h posttransfection, stained with NP-specific antibodies, and analyzed by confocal microscopy. (*C*) HEK293 cells were transfected with plasmids encoding all components for EBOV-specific minigenome assay and with plasmids encoding VP40 or VP40-TagRFP or a mixture of VP40-TagRFP and VP40, or without these plasmids (control). The negative control was without expression of L ( $\Delta$ L). At 48 h posttransfection, cells were lysed and the reporter gene activity was measured. The reporter gene activity in control cells was set to 100%. Lower show Western blot analysis to control protein expression by using NP-, TagRFP-, VP40-, and  $\alpha$ -tubulin-specific antibodies. (*D*) HEK293 cells were transfected with plasmids encoding all components of trVLP assay, either with wild-type VP40, or VP40-TagRFP, or with a mixture of VP40-TagRFP and VP40. At 72 h posttransfection, the cells were lysed, trVLPs were purified from the cell supernatant, and analyzed by Western blot using NP-, TagRFP-, VP40-, and  $\alpha$ -tubulin-specific antibodies.

**Table S1. Primer sequences**

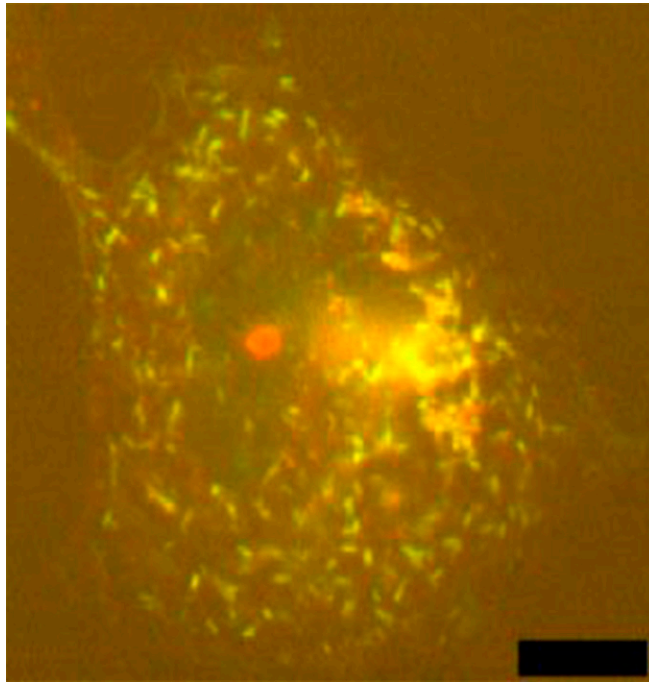
Primer name	Used for construct	Orientation	Sequence
4089 pCAGGS-TagRFP-fragment2-F	pCAGGS-VP24-TagRFP pCAGGS-VP40-TagRFP pCAGGS-NP-TagRFP	Forward	ggctcagggtcagggtccggctcagggtcagggtcctcagggtccatggtgtctaagggcgaaga
4090 pCAGGS-TagRFP-fragment2-R	pCAGGS-VP24-TagRFP pCAGGS-VP40-TagRFP pCAGGS-NP-TagRFP	Reverse	gttcggagcggccgctaattaagttgtgccca
4095 pCAGGS-VP24-fragment1-F	pCAGGS-VP24-TagRFP	Forward	gttcggaccgggatggctaagctacgggacg
4097 pCAGGS-VP24-fragment1-R	pCAGGS-VP24-TagRFP	Reverse	ggaccctgaggacctgaacctgagccgacctgaacctgagccgatagcaagagagctattaa
4100 pCAGGS-VP35-fragment1-F	pCAGGS-VP35-GFP	Forward	gttcggaccgggatgacaactagaacaagg
4101 pCAGGS-VP35-fragment1-R	pCAGGS-VP35-GFP	Reverse	ggaccctgaggacctgaacctgagccggacctgaacctgagccaattttgagtcgaagtgtt
4164 pCAGGS-GFP-fragment2-F	pCAGGS-VP35-GFP	Forward	ggctcagggtcagggtccggctcagggtcagggtcctcagggtccatggtgagcaagggcgagga
4127 pCAGGS-GFP-fragment2-R	pCAGGS-VP35-GFP	Reverse	gttcggagctagcttaagagctcggccgccc
4162 pCAGGS-VP40-fragment1-F	pCAGGS-VP40-TagRFP	Forward	gttcggaccgggatgagcgggttatattgcc
4163 pCAGGS-VP40-fragment1-R	pCAGGS-VP40-TagRFP	Reverse	ggaccctgaggacctgaacctgagccgacctgaacctgagccttctcaatcacagctggaa
4087 pCAGGS-NP-fragment1-F	pCAGGS-NP-TagRFP	Forward	gttcggaccgggatggattctgtctcagaaaa
4088 pCAGGS-NP-fragment1-R	pCAGGS-NP-TagRFP	Reverse	ggaccctgaggacctgaacctgagccggacctgaacctgagcctgatgatgttcaggattg



**Movie S1.** Transport of nucleocapsids labeled with VP35-GFP. Huh-7 cells expressing VP35-GFP were infected with EBOV, and analyzed by time-lapse microscopy at 24 h postinfection. One hundred frames were taken every 1 s. (Scale bar, 10  $\mu$ m.)

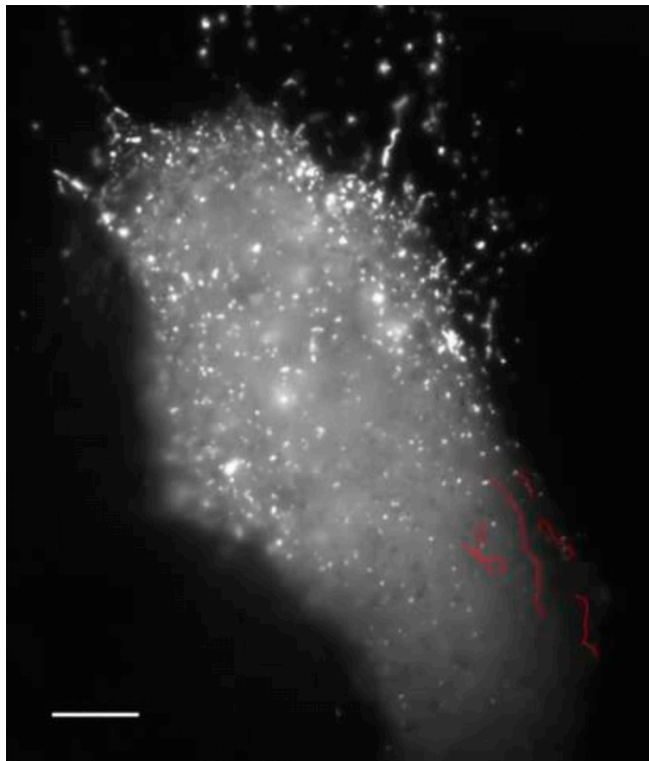
[Movie S1](#)





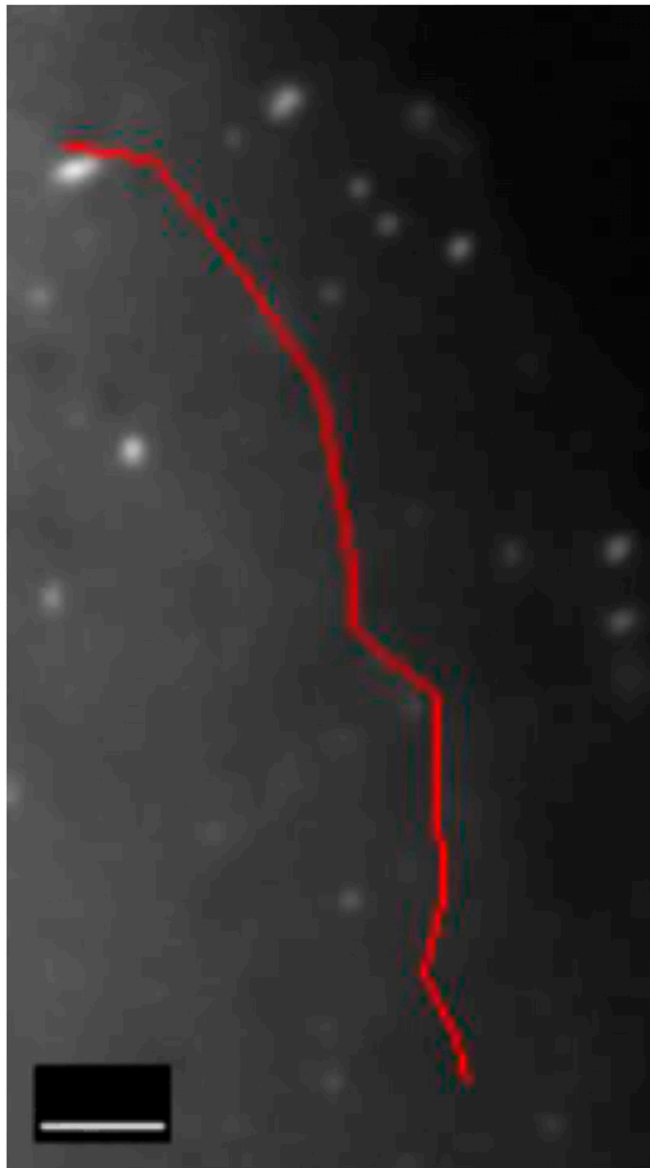
**Movie S2.** Transport of nucleocapsids labeled with VP30-GFP and VP24-TagRFP. Huh-7 cells expressing VP30-GFP and VP24-TagRFP were infected with EBOV, and analyzed by time-lapse microscopy at 24 h postinfection. One hundred frames were taken every 1.5 s. (Scale bar, 10  $\mu\text{m}$ .)

[Movie S2](#)



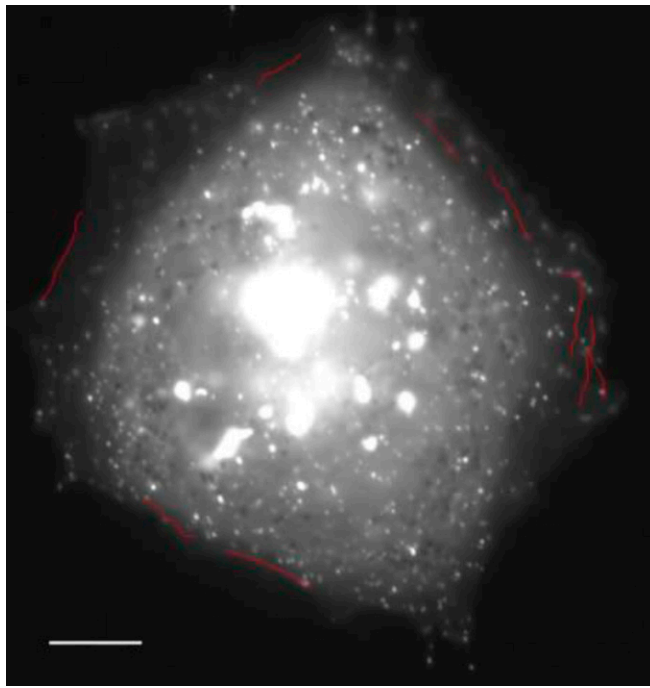
**Movie S3.** NCLSs transport in cells expressing all components of trVLP assay. Huh-7 cells were transfected with plasmids encoding VP30-GFP and all components of trVLP assay, and analyzed by time-lapse microscopy at 20 h posttransfection. Frames were acquired every 2 s for 2 min. (Scale bar, 10  $\mu\text{m}$ .)

[Movie S3](#)



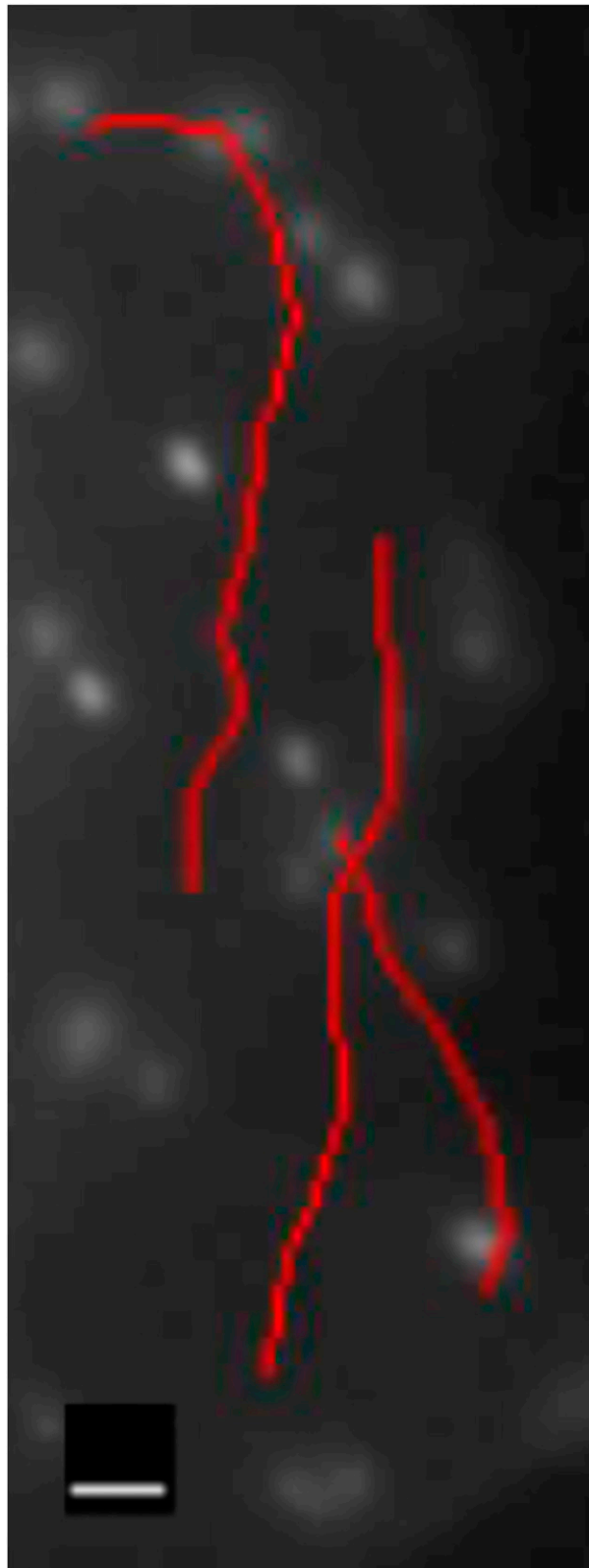
**Movie S4.** NCLSs transport in cells expressing all components of trVLP assay, cropped from Movie S3. The red line indicates trajectory of NCLS. Long-distance transport of NCLSs at higher magnification. (Scale bar, 2  $\mu\text{m}$ .)

[Movie S4](#)



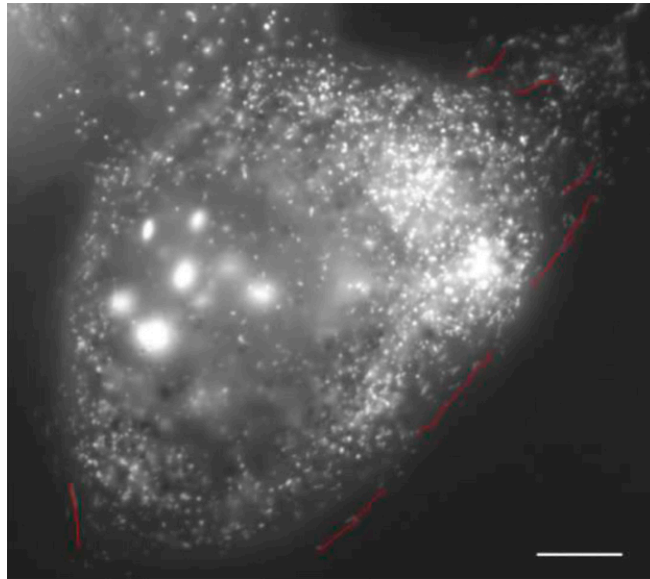
**Movie S5.** NCLs transport in cells expressing the nucleocapsid components. Huh-7 cells were transfected with plasmids encoding VP30-GFP and the nucleocapsid components (NP, VP35, VP24, L, minigenome, and T7 polymerase), and analyzed by time-lapse microscopy at 20 h posttransfection. Frames were acquired every 2 sec for 2 min. (Scale bar, 10  $\mu\text{m}$ .)

[Movie S5](#)



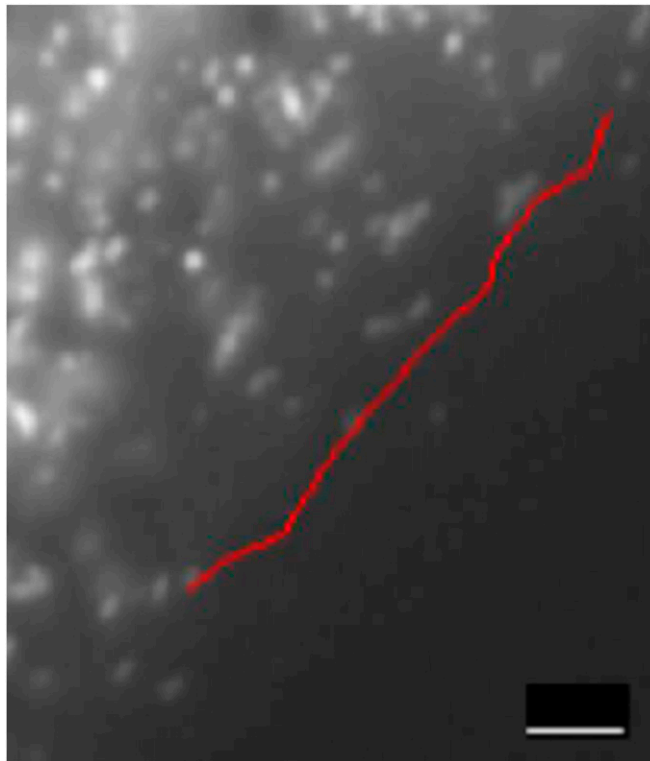
**Movie S6.** NCLSs transport in cells expressing the nucleocapsid components, cropped from Movie S5. Long-distance transport of NCLSs at higher magnification. The red lines indicate trajectories of NCLSs. (Scale bar, 2  $\mu\text{m}$ .)

[Movie S6](#)



**Movie S7.** NCLSs transport in cells expressing NP, VP35 and VP24. Huh-7 cells were transfected with plasmids encoding VP35-GFP, VP35, NP, and VP24, and analyzed by time-lapse microscopy at 20 h posttransfection. Frames were taken every 3 s for 2 min. (Scale bar, 10  $\mu\text{m}$ .)

[Movie S7](#)



**Movie S8.** NCLSs transport in cells expressing NP, VP35 and VP24, cropped from Movie S7. Transport of NP-, VP35-, and VP24-formed NCLSs at higher magnification. The red lines indicate trajectories of NCLSs. (Scale bar, 2  $\mu\text{m}$ .)

[Movie S8](#)